AIP Journal of Applied Physics

Triple-crystal x-ray diffraction analysis of reactive ion etched gallium arsenide

V. S. Wang, R. J. Matyi, and K. J. Nordheden

Citation: Journal of Applied Physics **75**, 3835 (1994); doi: 10.1063/1.356062
View online: http://dx.doi.org/10.1063/1.356062
View Table of Contents: http://scitation.aip.org/content/aip/journal/jap/75/8?ver=pdfcov
Published by the AIP Publishing

Articles you may be interested in
Time-Resolved X-Ray Triple-Crystal Diffractometry Probing Dynamic Strain in Semiconductors
AIP Conf. Proc. **879**, 1258 (2007); 10.1063/1.2436293

X-ray crystal truncation rod scattering analysis of reactive ion etched silicon
J. Appl. Phys. **84**, 5482 (1998); 10.1063/1.368311

High-resolution triple-crystal x-ray-diffraction experiments performed at the Australian National Beamline Facility in Japan (abstract)
Rev. Sci. Instrum. **66**, 1483 (1995); 10.1063/1.1145947

Triple crystal x-ray diffraction analysis of chemical-mechanical polished gallium arsenide
J. Appl. Phys. **72**, 5158 (1992); 10.1063/1.351995

High resolution x-ray diffraction analysis of annealed low-temperature gallium arsenide
Appl. Phys. Lett. **60**, 2642 (1992); 10.1063/1.106881

APL Photonics is pleased to announce Benjamin Eggleton as its Editor-in-Chief

[This article is copyrighted as indicated in the article. Reuse of AIP content is subject to the terms at: http://scitation.aip.org/termsconditions. Downloaded to] IP: 129.237.46.99 On: Mon, 16 Nov 2015 16:33:54

Triple-crystal x-ray diffraction analysis of reactive ion etched gallium arsenide

V. S. Wang
Materials Science Program, University of Wisconsin, Madison, Wisconsin 53706

R. J. Matyi
Department of Materials Science and Engineering, University of Wisconsin, Madison, Wisconsin 53706

K. J. Nordheden
Martin Marietta Electronics Laboratory (formerly GE Electronics Laboratory), Syracuse, New York 13221

(Received 12 October 1992; accepted for publication 19 October 1993)

The effect of BCl_3 reactive ion etching on the structural perfection of GaAs has been studied with diffuse x-ray scattering measurements conducted by high-resolution triple-crystal x-ray diffraction. While using a symmetric 004 diffraction geometry revealed no discernible differences between etched and unetched samples, using the more surface-sensitive and highly asymmetric 113 reflection revealed that the reactive ion etched samples etched displayed less diffusely scattered intensity than unetched samples, indicating a higher level of structural perfection. Increasing the reaction ion etch bias voltage was found to result in decreased diffuse scattering initially, until an apparent threshold voltage was reached, after which no further structural improvement was observed. Furthermore, we have shown that this reduction in process-induced surface structural damage is not due merely to the removal of residual chemical-mechanical polishing damage.

I. INTRODUCTION

Throughout the fabrication of advanced microelectronic devices and integrated circuits (ICs) on semiconductor materials, semiconductor substrates are subjected to numerous processes which may induce structural damage to surface and near-surface regions. Semiconductor wafer fabrication, wet chemical etching, plasma etching, metallization, and wafer cleaning are all common processes which may potentially alter the crystalline perfection of the substrate. Since the performance of these devices and circuits depends heavily upon the perfection of the substrate materials, such process-induced structural damage may create significant and adverse effects.

Reactive ion etching (RIE) has been increasingly used as a materials processing technique in compound semiconductor device and IC fabrication. The primary qualities that make RIE desirable for semiconductor processing include the ability to etch substrates anisotropically with the high dimensional resolution, etch uniformity, and material selectivity to produce the submicron-sized features required for state-of-the-art devices and ICs with ever-increasing performance and density specifications. RIE combines chemical processes due to the reaction between an etchant species and the substrate material, with mechanical processes due to the bombardment of the substrate surface by accelerated ions, photons, and electrons. It is the mechanical processes in RIE that contribute the most to surface and subsurface structural damage. RIE-induced radiation damage to GaAs surfaces has been found to cause reduced Schottky barrier heights and to decrease surface carrier concentrations.[1,2]

While many investigations of process-induced surface damage in GaAs have made use of electrical measurements which are quite sensitive to surface crystallographic imperfections, a structural probe is necessary to determine the mechanisms through which various processing techniques induce damage, and to correlate changes in electrical characteristics to specific structural defects. There is an intrinsic problem in characterizing the structural defects following a process such as RIE, however, since fabrication techniques are specifically designed to introduce as little damage into the semiconductor surface as possible. Thus, the analysis of defects generated by a nominally "damage-free" process would be expected to be somewhat difficult, even though such defects may significantly affect circuit performance.

X-ray diffraction has long been utilized to characterize structural defect in crystalline materials. Traditional x-ray diffraction techniques such as conventional double-crystal diffraction are primarily bulk materials characterization tools. Attempts to use these conventional methods to analyze thin surface layers often prove to be ineffective since the diffracted intensities from these layers can be negligible compared to the intense scattering generated by the bulk crystal. The total diffracted intensity measured in any x-ray diffraction experiment consists of two components: the dynamic, or perfect crystal contribution, and the kinematic, or imperfect crystal contribution, where crystal imperfection is caused by point defects and dislocations. In conventional double-crystal x-ray diffraction (DCD) with a parallel, nondispersive configuration $(+n,-n)$, these two components are convoluted, masking quantitative information that can be determined from either individual component alone. However, among several novel x-ray diffraction techniques that have been devised recently is that of triple-crystal diffraction (TCD). In TCD, with a $(+n,-n,+n)$

 0021-8979/94/75(8)/3835/7/$6.00 © 1994 American Institute of Physics

[This article is copyrighted as indicated in the article. Reuse of AIP content is subject to the terms at: http://scitation.aip.org/termsconditions. Downloaded to] IP: 129.237.46.99 On: Mon, 16 Nov 2015 16:33:54

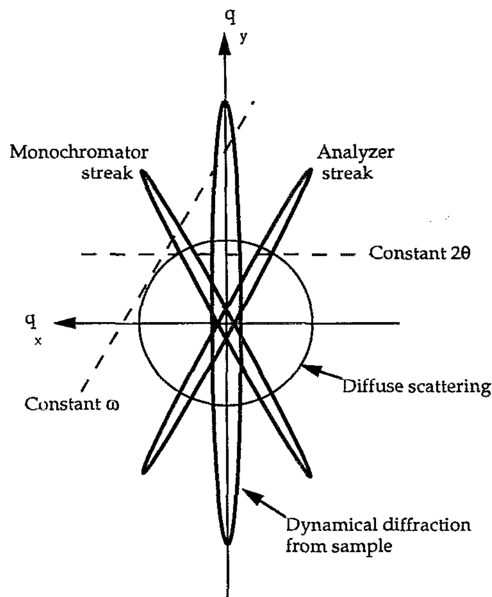

FIG. 1. Schematic illustration of the intensity distribution in reciprocal space as observed in a triple-crystal diffraction experiment.

configuration, a third crystal (the analyzer crystal) is inserted between the sample and the detector. By varying the angular positions of the sample and analyzer crystals at and near their exact Bragg conditions, it is possible to map the total diffracted intensity around a reciprocal lattice point, thus providing a means of direct and separate measurement of the dynamic and the kinematic diffraction components.[3,4] Using TCD, the diffracted intensity distribution in reciprocal space can be represented schematically by the diagram in Fig. 1. This characteristic pattern includes three streaks due to dynamical diffraction. The main "surface streak," or crystal truncation rod, is the result of strong scattering by the sample crystal and the termination of the crystal lattice at the sample surface.[5] The two additional "pseudo streaks" are due to similar singular reflections off the monochromator and the analyzer crystals. These pseudo streaks can be effectively eliminated by the use of multireflection grooved crystals, which produce essentially tailless beams.[6] Finally, any diffuse scattering present is centered around the reciprocal lattice point. Hence, the primary advantage of using TCD is the ability to directly analyze the kinematic diffuse x-ray scattering in the immediate vicinity of a reciprocal lattice point, independent of the dynamically scattered background.

Diffuse x-ray scattering is ideally suited for the investigation of structural defects in crystals, since the very reason diffuse scattering exists is due to the presence of these defects. In a "perfect" crystal, where all atoms are located precisely at their theoretical positions for a given lattice type, x rays are scattered only under a few discrete conditions, i.e., only at the exact Bragg reflections, and the atomic scattering amplitudes between these Bragg reflections are completely suppressed by destructive interference. In more realistic crystalline materials, defects such as vacancies, interstitials, point defect agglomerations, and dislocations are always present which distort the lattice planes from their ideal positions. Consequently, the scattered intensities at the exact Bragg conditions decrease, and the scattering amplitudes between Bragg peaks do not completely cancel out to zero. A *diffusely* scattered intensity is present which arises from two factors: scattering from the defects themselves, and scattering from the displacement disorder of the nonideal, distorted lattice.[7]

While the first theoretical calculations of diffuse scattering from crystals were conducted by Eckstein[8] and Huang[9] in the 1940s, only in more recent years as more high-powered x-ray sources and greater resolution experimental techniques and equipment have been developed has diffuse x-ray scattering been employed experimentally to study defects in crystal structures. Becker *et al.*[10] and Alexandropoulos and Kotsis[11] have measured changes in diffracted intensities due to mechanical polishing of Ge and Si, respectively, while Yasuami and Harada[12] and Kashiwagura *et al.*[13] have observed diffuse scattering in Si due to residual chemical-mechanical (CM) polishing. Several groups have also investigated the effects of ion implantation in Si[14,15] and GaAs[16] on the diffracted x-ray intensities. Recent high-resolution x-ray diffraction work involving defects in group III-V semiconductors include studies of bulk defects in InP by Gartstein[17] and near-surface defects in molecular beam epitaxy (MBE) grown GaAs by Bloch and co-workers.[18] We have previously reported on several high-resolution x-ray diffraction investigations regarding CM polish-induced damage to GaAs, including surface strain determination via precise lattice parameter measurements using grazing incidence diffraction (GIXD) and inclined Bragg plane diffraction (IBXD),[19] TCD measurements with the surface-sensitive IBXD geometry,[20] and diffuse scattering measurements using TCD.[21] Our studies on CM polishing of GaAs revealed the effects of individual CM polishing parameters on near-surface structural perfection as well as those of multiparameter interactions, leading to a better understanding of the underlying microscopic mechanisms of the CM polishing process. This body of prior work involving diffuse scattering measurements on semiconductor materials suggests that TCD is an ideal technique for monitoring the evolution of crystallographic damage in GaAs due to RIE processes.

II. EXPERIMENTAL

The GaAs samples used in this study were obtained from wafers CM polished by the vendor, and were nominally oriented 2° off ⟨001⟩ about the ⟨110⟩ axis. Immediately prior to loading into the RIE system, the GaAs samples were solvent cleaned, and dipped in 1:10 HCl:deionized H_2O for oxide removal. All plasma etching was conducted in a PlasmaTherm 2482 RIE system equipped with a 22 in. diameter electrode. The reactive etch species was introduced by BCl_3 gas at a flow rate of 14 sccm, and He gas was added to the etch chamber at 6 sccm. The resultant chamber pressure was 3.2 mTorr, and the bias voltage on the electrode and the total etch times were varied.

[This article is copyrighted as indicated in the article. Reuse of AIP content is subject to the terms at: http://scitation.aip.org/termsconditions. Downloaded to] IP: 129.237.46.99 On: Mon, 16 Nov 2015 16:33:54

The x-ray diffraction analyses were conducted using a Bede 150 double-crystal diffractometer which was modified for the TCD geometry.[22] Two grooved Si crystals, aligned for four (220) reflections in a (−,+,+,−) configuration, were used to monochromate the incident x-ray beam, and the cross-sectional area of the incident x-ray beam was ~2 mm^2. A triple-bounce (220) grooved Si crystal was used to analyze the total diffracted intensity from the sample crystal.[3,4,22] As previously noted, the use of these multiple-bounce crystals provides tailless beams, resulting in diffraction patterns that are free of dynamic scattering effects from the monochromator and analyzer crystals. Due to the slight misorientation of the GaAs substrates, it was necessary to mount the samples in such a manner that the substrate misorientation direction was contained within the plane of the diffractometer in order to maintain a consistent x-ray optical configuration. A Rigaku RU200 rotating anode generator provided Cu $K\alpha_1$ radiation. The x-ray generator power used for the TCD scans was 50 kV and 200 mA.

In order to measure the total diffracted intensity around a reciprocal lattice point using TCD, scans were conducted by rocking the sample crystal while keeping the analyzer crystal in a fixed position, incrementing the analyzer crystal position, then scanning the sample crystal again with the analyzer fixed. The incremental step sizes used for the sample and the analyzer crystals were 6 and 12 arcsec, respectively. This procedure was followed until the diffracted intensities in a trapezoidal region surrounding the reciprocal lattice point was mapped out in reciprocal space. Real space diffractometer coordinates were converted to the reciprocal space coordinates (q_x,q_y) using the relations of Iida and Kohra,[6] where the $\mathbf{q}_y$ direction is parallel to the direction of the reciprocal lattice vector of the diffracting planes and the $\mathbf{q}_x$ direction is orthogonal to $\mathbf{q}_y$. A typical parasitic count rate of about 0.5 counts/s (which includes 0.2 counts/s due to electrical noise in the detector) was achieved by shielding both the analyzer crystal and the scintillation detector in order to reduce background scatter, and the total count time per step was 10 s. Further details of this experimental setup have been previously described in greater detail elsewhere.[21,22]

III. RESULTS

Figures 2(a) and 2(b) display the diffracted intensities measured about the 004 reciprocal lattice point for an unetched GaAs sample (sample 4A) which was chemical-mechanical (CM) polished by the vendor and a reactive ion etched GaAs sample (sample 4B), respectively. For the RIE-treated sample, a bias voltage of −250 V was used, and the total etch time was 15 min, resulting in an etch depth of ~1000 Å. The TCD scans illustrated in the figure display the two primary characteristics which were observed in all of the measurements made in this investigation. As discussed earlier, the crystal truncation rod, or surface streak, is present which extends along the $\mathbf{q}_y$ direction in reciprocal space in this case, and is a dynamic diffraction effect caused by the termination of the crystal at the sample surface. In addition to this surface streak, kinematic diffuse x-ray scattering generated by crystal defects is also visible in the intensity maps, and is distributed around the reciprocal lattice points. The data shown in Fig. 2 and in all subsequent triple crystal scans were contoured using the logarithm of the diffracted intensity, with each contour denoting an intensity increment of $10^{0.25}$ counts/s. The minimum contour level was a log (intensity) of 0.25, corresponding to ~1.8 counts/s, which significantly exceeds the parasitic background level previously discussed.

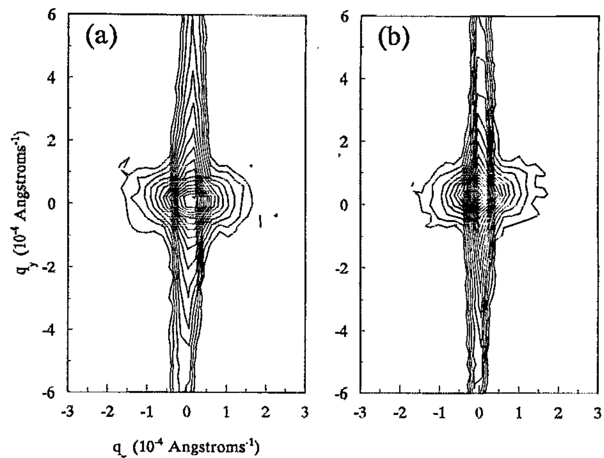

FIG. 2. 004 triple-crystal scans from (a) GaAs sample 4A (no RIE) and (b) sample 4B (RIE, −250 V bias voltage). Identical ranges of $\mathbf{q}_x$ and $\mathbf{q}_y$ are used in all scans.

Upon initial inspection, the similarities between the diffuse scattering profiles from the CM polished and the plasma-etched GaAs samples seemed to suggest that the magnitude of any crystallographic damage induced by the RIE process was likely to be very small. While this may indeed have been the case, the surface sensitivity of similar x-ray measurements conducted previously on chemical-mechanical polished GaAs[21] indicated that though small, the surface damage should be measurable by TCD.

The diffraction profiles illustrated in Fig. 2 were recorded using the 004 reflection, which is symmetrical with respect to the sample surface. However, the 004 reflection is also characterized by a relatively large x-ray photoelectric penetration depth (as calculated from kinematic theory) of 15.5 μm for 90% absorption of Cu $K\alpha$ x rays in GaAs. Alternatively, a highly asymmetric reflection such as the 113 reflection reduces the 90% absorption depth for Cu $K\alpha$ x rays in GaAs to 1.5 μm.[23] Thus, the use of an asymmetric reflection such as the 113 reflection offers the prospect of an increased sensitivity to plasma etch-induced surface damage. Figure 3 compares the symmetric 004 and the asymmetric 113 diffraction geometries by schematically illustrating the relationships between the monochromator, sample, and analyzer crystals, and the wave vectors $\mathbf{S}_0/\lambda$ and $\mathbf{S}/\lambda$ of the incident and diffracted beams. For the 004 diffraction scans, the surface streak will be oriented exactly parallel to the $\mathbf{q}_y$ direction, or along the $\mathbf{H}^*_{004}$ direction in reciprocal space. However, when the diffracted intensities

[This article is copyrighted as indicated in the article. Reuse of AIP content is subject to the terms at: http://scitation.aip.org/termsconditions. Downloaded to] IP: 129.237.46.99 On: Mon, 16 Nov 2015 16:33:54

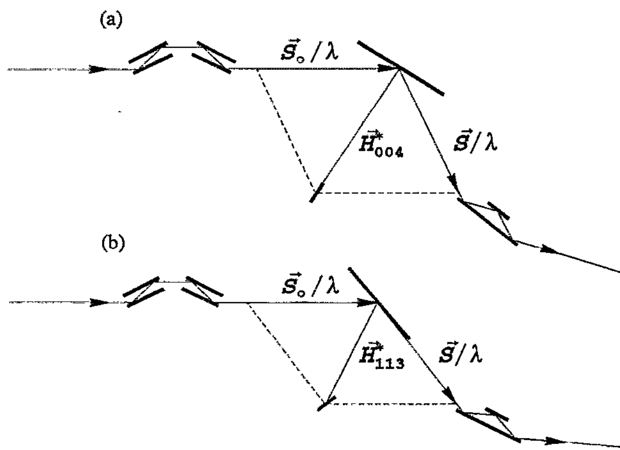

FIG. 3. Triple-crystal diffraction geometries for (a) the symmetric 004 reflection and (b) the asymmetric 113 reflection, schematically illustrating the four reflection monochromator, the sample crystal, and the three reflection analyzer crystal. Also shown are the incident and diffracted wave vectors $\mathbf{S}_0/\lambda$ and $\mathbf{S}/\lambda$ and their relation to the reciprocal lattice vector $\mathbf{H}^*_{hkl}$.

are mapped around the 113 reciprocal lattice points, the crystal truncation rod will be tilted by an amount equal to the angle formed between the diffracting planes and the sample surfaces, which, for the case of the 113 reflection in an 001 GaAs substrate, is 25.23°. Thus, while the orientation of the diffraction planes always remains constant with respect to the frame of reference of the (q_x,q_y) coordinate system in reciprocal space regardless of the reflection being used, the orientation of the dynamically diffracted surface streak changes with the orientation of the sample surface.

TCD maps of diffracted intensity in reciprocal space around the 113 reciprocal lattice point were then recorded for the same two samples analyzed above for the 004 reciprocal lattice point. Figure 4 displays the diffracted intensities obtained from the 113 reflections for both the CM-polished and the RIE-treated samples. The surface streaks are still present, although as expected they are no longer oriented along the $\mathbf{q}_y$ direction as in the symmetrical geometry case. However, unlike in the symmetrical case, a difference in the magnitude of diffuse scattering was observed between the unetched and the plasma-etched samples. Quite unexpectedly, a *greater* amount of diffuse scattering, was found in the CM-polished sample than in the plasma-etched sample. As shown in Fig. 4, the maximum extent of the diffuse scattering in the $\mathbf{q}_x$ direction at the level of the minimum contour decreased from 2.4×10^{-4} to 2.0×10^{-4} Å^{-1} from the CM-polished samaple to the RIE sample. Therefore, it appeared that the RIE process employed either decreased or removed residual surface structural damage associated with conventional CM polishing procedures used in GaAs wafer fabrication. This was an extremely surprising result, since processing techniques such as RIE are typically viewed as being *sources* of crystallographic damage as opposed to being means of defect removal.

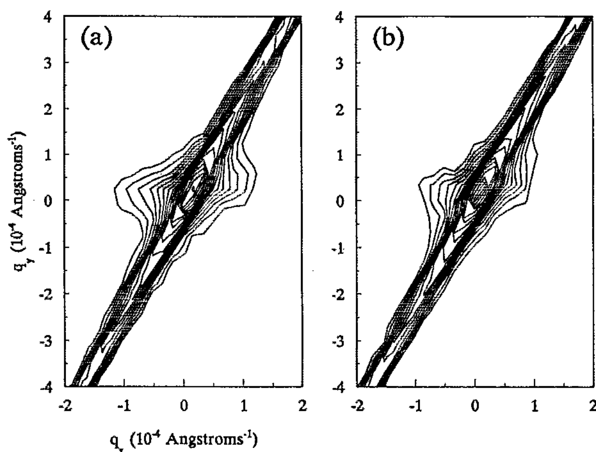

FIG. 4. 113 triple-crystal scans from (a) sample 4A (no RIE) and (b) sample 4B (RIE, −250 V bias voltage).

From these intriguing results, it was not possible to determine if the diffuse scattering after RIE decreased because the concentration of defects was actually being reduced, or if a damaged layer remaining from the CM polishing process was simply being etched away, resulting in a diffraction profile which merely reflected the bulk defect concentration instead of a reduced surface defect level. Previous reports have indicated the presence of such residual CM polish damage in GaAs.[19–21] In order to differentiate between these two possible situations, another set of RIE experiments was conducted. Before the samples were plasma etched, they were all wet chemically etched in a solution of 3:1:1 H_2SO_4:H_2O_2:H_2O. Nearly 2.5 μm was removed from each sample to insure that any residual structural damage resulting from CM polishing was completely eliminated. The RIE procedures were identical to those described above, except for the total etch times, which were 30 min per sample, and the bias voltages. Sample 5A was plasma etched using a bias voltage of −115 V, and sample 5B was etched at −460 V. Sample 5C was used as the control sample, and was not eteched by RIE.

Again, the diffuse scattering around the 113 reciprocal lattice point was measured for each sample with the asymmetric TCD geometry used previously. The resultant diffracted intensity maps in reciprocal space are shown in Fig. 5. Figures 5(a), 5(b), and 5(c) display the TCD results from the control sample, the sample plasma etched at a bias voltage of −115 V, and the sample etched at −460 V, respectively. As with the first set of RIE samples, the same trends existed in the lateral extent (in the $\mathbf{q}_x$ direction) of the diffuse scattering. As the bias voltage was increased, effectively increasing the energy of the ions bombarding the sample surfaces, the amount of diffuse scattering decreased, indicating a more perfect crystalline structure in the near surface regions.

IV. DISCUSSION

The primary benefit of using TCD analysis to examine surface and near-surface structural perfection is readily apparent from the contour plots of total diffracted intensities. The capability of TCD to plot the intensity distribution

[This article is copyrighted as indicated in the article. Reuse of AIP content is subject to the terms at: http://scitation.aip.org/termsconditions. Downloaded to] IP: 129.237.46.99 On: Mon, 16 Nov 2015 16:33:54

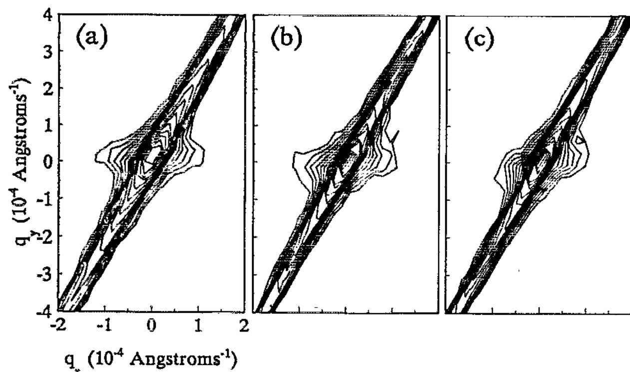

FIG. 5. 113 triple-crystal scans from (a) sample 5C (no RIE), (b) sample 5A (RIE, −115 V bias voltage), and (c) sample 5B (RIE, −460 V bias voltage). All samples were wet chemically etched in a 3:1:1 H_2SO_4:H_2O_2:H_2O solution to remove residual polish damage prior to plasma etching.

around a reciprocal lattice point, i.e., creating an intensity "map" in reciprocal space, allows for direct and immediate observation of changes in the diffuse scattering. In contrast, conventional double-crystal diffraction with no analyzer crystal and a wide open detector results in an integration of intensities across the surface of the diffracting crystal's Ewald sphere.[6] In reciprocal space, this condition corresponds to simultaneously recording all of the diffracted intensity along a line inclined by $90° - \theta_B$ with respect to the $\mathbf{q}_x$ direction, where θ_B is the exact Bragg angle of the sample's diffracting planes. Therefore, the typically weak diffuse scattering is superimposed upon the much stronger surface streak intensity. Thus, DCD rocking curves generally reveal only the $1/q^2$ relationship between diffracted intensity and deviations from the exact Bragg angle that is accounted for by the dynamically diffracted surface streak.

It should be noted that in the case of the asymmetric reflection, the diffracted beam formed a nearly grazing angle with the sample surface (i.e., a "grazing exit" geometry) as opposed to having the incident x-ray beam form a nearly grazing angle with the sample surface ("grazing incident" geometry). This grazing exit experimental arrangement simplified the physical positioning of the sample crystal by reducing the effects of centering errors. Furthermore, using the grazing exit diffracted beam served to reduce the size of the beam emerging from the sample crystal. Had a grazing incident beam been used, the spatially expanded diffracted beam would have been larger than the acceptance aperture of the grooved three-reflection analyzer crystal, and valuable intensity would have been lost.

Although the intensity distribution maps resulting from the TCD measurements are extremely useful and simple to use to analyze structural changes in a qualitative sense, far more information on the mechanisms of RIE surface structure modification could be obtained by a more quantitative analysis. More specifically, it would be very beneficial to correlate RIE process-induced damage to a single parameter which quantifies the amount of the kinematically scattered diffuse intensity due to structural imperfections. This parameter has been defined as an excess intensity, I_{excess}, which is the amount of diffracted intensity present in addition to the dynamically scattered surface streak, and has been discussed in detail previously.[21] Since the total diffracted intensity is present throughout a volume of reciprocal space, I_{excess} can be calculated by performing a cylindrical integration of the scattered intensity according to the relation[24]

$$I_{\text{excess}} = 4\pi \int \int I_{\text{net}}(q_x, q_y) q_x \, dq_x \, dq_y. \quad (1)$$

The net intensity, $I_{\text{net}}(q_x, q_y)$, is defined as the diffracted intensity above an arbitrarily designated minimum level. For this study, this minimum intensity level was chosen to be the minimum contour level used in all of the intensity distribution maps, i.e., $10^{0.25}$, or about 1.8 counts/s. In the direction parallel to the reciprocal lattice vector of the (113) diffracting planes, the limits of integration were taken to be $\pm q_{y,\text{max}}$, representing the overall range that was scanned in reciprocal space, which, in the case of all of the scans conducted in this investigation, corresponded to 720 arcsec in real space. In the direction perpendicular to the 113 reciprocal lattice vector, the integration was performed from $2.35 r_0$ [$\approx r_0/\sin 25.23°$, where 25.23° is the angle between the diffracting (113) planes and the (001) GaAs substrate] to $q_{x,\text{max}}$, the limit of the reciprocal space scan in the $\mathbf{q}_x$ direction. Therefore, a "radius" of the surface streak r_0 is defined which excluded the intensities along the surface streak from the calculation of I_{excess}. If a data point was located within r_0 of a straight line along the center of the surface streak, then it was considered to be part of the surface truncation rod, and was excluded from the diffuse scattering calculation. In all of the calculations performed for this study, r_0 was chosen to be 0.5×10^{-4} Å^{-1}. Using this surface streak subtraction procedure, an ideally perfect crystal should have an I_{excess} of zero if the correct surface streak radius is chosen. We have indeed verified this using a highly perfect Ge crystal which was grown with no detectable dislocations, was not intentionally doped, and was polished and extensively etched to remove all traces of surface damage. Figure 6 shows a TCD scan performed on this sample using the 113 reflection. Obviously, this germanium crystal does not possess the relatively high level of intrinsic grown-in defects found in GaAs, as evidenced by the lack of diffuse scattering. Quantitatively, this fact is borne out by calculations in which I_{excess} equals zero for a surface streak radius r_0 of 0.48×10^{-4} Å^{-1}. Thus, the procedure and the r_0 selected for the current study both appear to be reasonable and appropriate choices.

Table I lists the results of the excess intensity calculations for both of the RIE-treated sample groups examined in this study. In each case, the integrated intensities shown are given in arbitrary units which have been normalized to the excess intensity of the respective control sample. For samples 4A and 4B, which were not free-etched prior to RIE, the excess diffuse intensity after plasma etching at a bias voltage of −250 V decreased to 37% of the diffuse intensity of the untreated sample. This was the initial result

[This article is copyrighted as indicated in the article. Reuse of AIP content is subject to the terms at: http://scitation.aip.org/termsconditions. Downloaded to] IP: 129.237.46.99 On: Mon, 16 Nov 2015 16:33:54

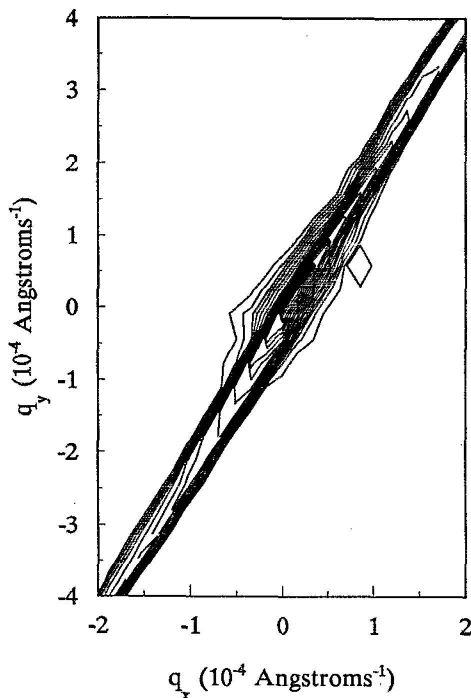

FIG. 6. 113 triple-crystal scan from highly perfect Ge.

that triggered the hypothesis that perhaps the RIE was simply removing residual CM-polish damage from the GaAs surface. However, when the second group of samples was analyzed (samples 5A, 5B, and 5C, which were free-etched prior to any RIE to remove any residual CM-polish damage), the identical trends were found. Compared to the diffuse intensity of the control sample, the sample plasma eteched at a bias voltage of −115 V (sample 5A) showed a 19% decrease in excess intensity. Sample 5B, which was subjected to RIE at a bias voltage of −460 V, displayed an excess diffuse intensity of only 42% of that for the control sample. These results confirmed that the BCl_3 RIE process employed in this investigation did indeed improve the structural perfection of the GaAs samples treated.

TABLE I. Relative excess integrated intensity measurements from reactive ion etched GaAs. Sample 5 was wet chemically etched in a 3:1:1 H_2SO_4:H_2O_2:H_2O solution prior to RIE, while sample 4 received no prior wet chemical etch. The center columns are integrated intensities in arbitrary units calculated from Eq. (1), while the column on the right normalizes the calculated intensities to samples 4A and 5C.

Sample	Intensity from Eq. (1) (10^{-3} arb. units)	Normalized intensity
Perfect Ge	0	0
4A (no RIE)	5.62	1.00
4B (−250 V RIE)	2.10	0.37
5C (no RIE)	5.09	1.00
5A (−115 V RIE)	4.12	0.81
5B (−460 V RIE)	2.15	0.42

The data in Table I reveal some additional points. First, the absolute excess intensities (expressed in arbitrary intensity units) calculated for the two control samples were remarkably similar (5.62×10^{-3} for sample 4A vs 5.09×10^{-3} for sample 5C). This indicates that, contrary to the initial hypothesis, the diffuse scattering observed from sample 4A was not largely due to residual CM-polish damage, but rather could more accurately be attributed to the intrinsic grown-in defect structure of bulk GaAs. This fact also allowed for more direct comparisons between the plasma-etched samples from the two sample groups. For instance, the values of I_{excess} for samples 4B (−250 V) and 5B (−460 V) relative to the control samples were quite similar (0.37 for sample 4B, 0.42 for sample 5B). This result seems to indicate that for increasing bias voltages, the surface structure actually becomes less defective to a certain point, after which no further structural improvement is observed as the bias voltage is increased, i.e., some threshold voltage may exist.

A possible explanation for this phenomenon is that, at the higher voltages, there may be an etch rate limitation due to the deposition/redeposition of chemical reaction products, or that the chemical reactions themselves are being inhibited. Ion-assisted athermal crystallization is a well-known phenomenon,[25] and it is conceivable that such a process is occurring during reactive ion etching of GaAs. However, it is difficult to understand how an ion-assisted crystallization process could produce a surface layer of single-crystal (not polycrystalline) GaAs that has a structural perfection that is apparently superior to that of the original substrate material. While it is not possible at this stage to rigorously assign a mechanism to the structural changes observed, these results to inspire further investigations into possible phenomena such as dislocation annihilation in the GaAs substrates.

V. CONCLUSIONS

We have shown that high-resolution triple-crystal diffraction can be very effectively used to map the diffracted intensity distribution in reciprocal space around a reciprocal lattice point. Measurements obtained from this technique have been used to calculate an excess diffuse intensity, a parameter which can be directly correlated to structural perfection. Application of these calculations to GaAs samples plasma etched by a BCl_3 RIE process revealed the surprising result that the GaAs surface structure actually improved after RIE. Further x ray analyses as well as complementary electrical and chemical characterization techniques are being conducted to further elucidate the mechanisms involved.

ACKNOWLEDGMENTS

The authors gratefully acknowledge support from the National Science Foundation under Grants Nos. ECS-8908439 and DMR-8907372. We gratefully acknowledge discussions with Professor C. R. Aita (University of

[This article is copyrighted as indicated in the article. Reuse of AIP content is subject to the terms at: http://scitation.aip.org/termsconditions. Downloaded to] IP: 129.237.46.99 On: Mon, 16 Nov 2015 16:33:54

Wisconsin-Milwaukee) on athermal crystallization. One of us (VSW) acknowledges the support of a NDSEG fellowship.

[1] S. W. Pang, J. Electrochem. Soc. **133**, 784 (1986).
[2] T. Hara, H. Suzuki, A. Suga, T. Terada, and N. Toyoda, J. Appl. Phys. **62**, 4109 (1987).
[3] P. F. Fewster, J. Appl. Crystallogr. **22**, 64 (1989).
[4] P. F. Fewster, J. Appl. Crystallogr. **24**, 178 (1991).
[5] S. R. Andrews and R. A. Cowley, J. Phys. C **18**, 6427 (1985).
[6] A. Iida and K. Kohra, Phys. Status Solidi A **51**, 533 (1979).
[7] H. C. Haubold, Rev. Phys. Appl. **11**, 73 (1976).
[8] H. Eckstein, Phys. Rev. **68**, 120 (1945).
[9] K. Huang, Proc. R. Soc. London Ser. A **190**, 102 (1947).
[10] K. Becker, U. Winter, A. A. Zav'yalova, M. V. Kovalchuk, A. A. Lomov, and P. Zaumseil, Sov. Phys. Cryst. **29**, 525 (1984).
[11] N. G. Alexandropoulos and K. T. Kotsis, J. Appl. Crystallogr. **18**, 509 (1985).
[12] S. Yasuami and J. Harada, J. Appl. Phys. **52**, 3989 (1981).
[13] N. Kashiwagura, J. Harada, and M. Ogino, J. Appl. Phys. **54**, 2706 (1983).
[14] P. Zaumseil and U. Winter, Phys. Status Solidi A **120**, 67 (1990).
[15] A. Y. Kazimirov, M. V. Kovalchuk, and V. G. Kohn, Acta Crystallogr. Sect. A **46**, 643 (1990).
[16] P. A. Aleksandrov, A. A. Zav'yalova, and A. A. Lomov, Sov. Phys. Crystallogr. **29**, 386 (1984).
[17] E. L. Gartstein, Z. Phys. B **88**, 327 (1992).
[18] R. Bloch, D. Bahr, J. Olde, L. Brugemann, and W. Press, Phys. Rev. B **42**, 5093 (1990).
[19] V. S. Wang and R. J. Matyi, J. Electron. Mater. **21**, 23 (1992).
[20] V. S. Wang and R. J. Matyi, Mater. Res. Soc. Symp. Proc. **259**, 335 (1992).
[21] V. S. Wang and R. J. Matyi, J. Appl. Phys. **72**, 5156 (1992).
[22] R. J. Matyi, Rev. Sci. Instrum. **63**, 5591 (1992).
[23] M. A. G. Halliwell, Inst. Phys. Conf. Ser. (4th Int. Symp. on GaAs and Related Compounds) **17**, 98 (1973).
[24] R. J. Matyi and B. Crist, Jr., J. Polym. Sci. (Polym. Phys. Ed.) **16**, 1329 (1978).
[25] J. E. Greene, in *The Handbook of Crystal Growth, Vol. 1: Fundamentals*, edited by D. T. J. Hurle (Elsevier, Amsterdam, in press); S. Nikzad and H. A. Atwater, Mater. Res. Soc. Symp. Proc. **223**, 53 (1991).

[This article is copyrighted as indicated in the article. Reuse of AIP content is subject to the terms at: http://scitation.aip.org/termsconditions. Downloaded to] IP: 129.237.46.99 On: Mon, 16 Nov 2015 16:33:54